NUKLEONIKA 2001;46(2):63–69

ORIGINAL PAPER

Influence of gamma and proton radiations on the absorption, photoluminescence and birefringence of lithium niobate single crystals doped with Cu, Fe and Cr ions

Sławomir M. Kaczmarek

Abstract The results of investigations of the influence of gamma and proton radiations on absorption, luminescence and birefringence of either pure or Cu, Fe and Cr doped $LiNbO_3$ single crystals were presented. A method of birefringence dispersion testing on the entire areas of plane-parallel plates of $LiNbO_3$ crystals has been illustrated by the influence of both types of irradiation on pure and Fe, Cr and Cu-doped $LiNbO_3$ wafers. It was found that Li NbO_3 LN:Cu single crystal shows a different behavior compared with other investigated crystals. First of all it exhibits lower susceptibility to γ-rays, the absence of 500 nm additional absorption, and a strong proton susceptibility observed in polarimeter measurements.

Key words absorption • birefringence • gamma radiation • lithium niobate • proton radiation • wafers

Introduction

Metal oxides have a wide-ranging importance in many areas of physics and technology. They are applicable as ceramics, high-T_c superconductors or substrates for the latter and have relevance to microelectronics and especially for laser materials. Irradiation of these materials by energetic particles leads to recharging of existing point defects as well as to the displacement of atoms into interstitial positions, forming what is commonly called a Frenkel defect [7]. In the oxygen sublattice this could result in the formation of three kinds of Frenkel defect pairs: neutral interstitial O_j atom and V_o vacancy, or a vacancy with one or two trapped electrons (the so-called F^+ and F center) and their complementary O_j^- and O_j^{2-} defects. The current understanding of the defects in oxides has been given in [5].

A survey of recent theoretical studies of radiation-induced point defects in simple oxides with emphasis on highly ionic MgO, partly-covalent corrundum (Al_2O_3) and ferroelectric $KNbO_3$ has been presented in [14].

The influence of X-rays on the absorption spectrum of ferroelectric $LiNbO_3$, pure and doped with transition metal ions (Cu, Mn, Ni) was firstly investigated in [1]. Three main bands with peaks at 1.6 eV (polaron Nb^{4+}), 2.5 eV and 3.2 eV (holes trapped at Li vacancies) have been observed in pure crystals or Mn-, Ni- and Eu-doped crystals after low temperature (10 K) irradiation. For the Cu-doped samples, a competition is apparent between the production of these bands and the conversion of Cu^{2+} (1.2 eV band) into Cu^+ (3.1 eV band).

Some results of the investigations of influence of γ-rays on optical properties of $LiNbO_3$ and $LiTaO_3$ single crystals doped with transition metal ions were described in [5, 6].

S. M. Kaczmarek
Military University of Technology,
Institute of Optoelectronics,
2 Kaliski Str., 00-908 Warsaw, Poland,
Tel.: +4822/ 6839019, Fax: +4822/ 6668950,
e-mail: skaczmar@ack.wat.waw.pl

Received: 2 January 2001, Accepted: 14 March 2001

Under gamma irradiation there was stated the conversion of Cu^{2+} into Cu^{+} in $LiNbO_3$ doped with Cu [8] and a specific radiation defect in $LiNbO_3$ doped with Cr [10] (ESR spectra). In these papers some results of electron irradiations were also presented, especially ionization of Mn^{2+} to Mn^{3+} in a $LiNbO_3$ single crystal doped with Cr, in which Mn dopant was uncontrolled one.

Obviously one of the most important factors in radiation defect investigations to understand the nature of color and impurity centers in $LiNbO_3$ or $LiTaO_3$ perovskites is the stoichiometry of investigated crystals. Some interesting results on the color centers in stoichiometric $LiNbO_3$ single crystals one can find e.g. in [15, 18].

In this paper we present results of the influence of gamma and proton radiation on optical properties of either pure or Cu, Fe and Cr doped $LiNbO_3$ single crystals, whose initial state is congruent $Li_{0.98}Nb_{1.02}O_3$. The investigations were performed for samples with thickness and surface areas characteristic of optoelectronic devices (polarizers, Q-switches, retardation plates and others), and at temperatures characteristic of their job conditions.

Methods

$LiNbO_3$ single crystals were grown in Y direction by the Czochralski technique from the congruent melt (51.4 mol.% Li_2O:48.6 mol.% Nb_2O_5) in the Institute of Electronic Materials Technology [19]. Specimens of the following compositions were prepared: $LiNbO_3$ (LN), LN:Fe (0.1 at.%), LN:Cu (0.05 at.%, 0.06 at.% and 0.07 at.%), LN:Cr (0.3 at.%).

The samples were cut out from the crystals parallel to the Y growth direction, and perpendicular to Z and then polished to the thickness of about 3 mm. They were irradiated by gamma photons immediately after the crystal growth process. A ^{60}Co gamma source with a power of 1.5 Gy/sec was used. After annealing at 800°C in air for 5 h, samples were subsequently irradiated by protons (p^+) in the C30 cyclotron, the proton fluence was varied from 5×10^{12} to about 1.2×10^{16} protons/cm^2. To avoid overheating, the average beam current was kept at approximately 200 nA. Collimated to about 10 mm in diameter the external proton beam passed through the few cm long air gap, where the crystal samples were placed. The effective proton energy at the entrance face of the sample was ca. 21 MeV.

Optical transmission was measured before and after γ, p^+ and annealing treatments using a LAMBDA-900 Perkin-Elmer spectrophotometer in the UV-VIS range and FTIR-1725 in the IR range. Additional absorption due to the irradiation or annealing was calculated according to the formula:

$$\Delta K(\lambda) = (1/d)\ln(T_1/T_2) \quad (1)$$

where K is the absorption, λ is the wavelength, d is the sample thickness and T_1 and T_2 are the transmissions of the sample before and after a treatment, respectively. The transmission investigations were obtained at room temperature.

Photoluminescence caused by 514.5 nm argon laser excitation at 10 K was measured only for the LN:Cr single crystal. The luminescence spectrum was registered using a GDM-1000 monochromator and an EMI 9684B photomultiplier with the aim of checking the Cr^{3+} ions lattice position.

In such a way the samples have undergone a series of treatments including: gamma irradiation (10^5 Gy), thermal annealing (air, 400°C, 5 h), 2nd gamma irradiation (10^6 Gy), 2nd thermal annealing (air, 800°C, 5 h), 3rd gamma irradiation (10^7 Gy), and the final 3rd thermal annealing (air, 800°C, 5 h). At the end the crystals were irradiated with p^+ with fluences up to 1.2×10^{16} cm^{-2}.

Changes in the birefringence and birefringence dispersion coefficient were examined using the relation:

$$\mathrm{BRD} = \frac{\Delta n(\lambda_i)}{\Delta n(\lambda_{i+1})} \quad (2)$$

for λ = 670 nm step 10 nm.

A TV camera and video frame grabbing techniques were used for collecting the input data from the whole surface of the investigated wafer, and hence birefringence in homogeneity maps were obtained [2].

Results

Fig. 1 presents absorption measurements for three investigated crystals. As one can see fundamental absorption edge shifts towards longer wavelengths from 320 nm for pure LN by LN:Cr, LN:Fe to 420 nm for LN:Cu.

The absorption of the LN:Cr single crystal exhibits clear bands peaked at 464, 659, 731, 1265, and 2871 nm. Broadband absorption at 464 and 659 nm, respectively, corresponds to the transitions $^4A_2\rightarrow{}^4T_1$, $^4A_2\rightarrow{}^4T_2$. They occur in the red-orange and green-blue regions respectively, giving rise to the characteristic colors of Cr^{3+} doped crystals. The 731 nm band is an $^2E\rightarrow{}^4T_2$ transition giving rise to R lines, the 1265 nm band may be Cr^{4+} or Cr^{5+} absorption and the 2871 nm band is the absorption of OH^- ions.

The absorption of the LN:Fe shows transitions characteristic of Fe^{2+} peaked at 482 nm and 1062 nm [3]. The first is probably a Fe^{2+} d$\rightarrow$d transition which is assigned usually to $Fe^{2+}\rightarrow Nb^{5+}$ intervalence transfer, and the second is an $^5A\rightarrow\gamma E$ transition. Nevertheless, the shape of this band and the intensity of OH^- band at 2871 nm suggest the presence of Fe^{3+} ions.

The absorption of the LN:Cu shows a band at 460 nm which gives rise to the red-yellow color of the crystal, an asymmetric band peaked at about 1000 nm which at low temperatures exhibits triplet structure (878, 953 and 1109 nm), and the 2000 nm symmetric band. The 460 nm band may be connected with $Cu^{+}\rightarrow Nb^{5+}$ intervalence transfer, the 1000 and 2000 nm bands are $^2E\rightarrow{}^2T_2$ and ^2E transitions in Cu^{2+} [17].

The luminesence of the LN:Cr single crystal at low temperatures (Fig. 2) exhibits a broad emission band peaked at about 950 nm and R-lines peaked at 730.7 and 734.4 nm with linewidths of about 2 nm. The first line is connected

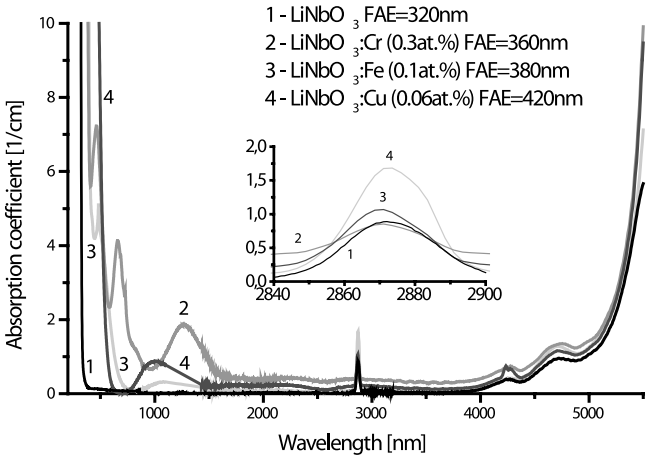

Fig. 1. Absorption curves of LN (1), LN:Cr (2), LN:Fe (3) and LN:Cu (4) single crystals.

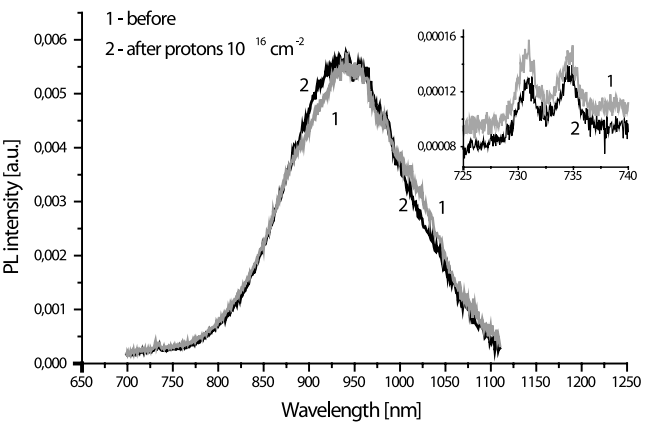

Fig. 2. Photoluminescence of LN:Cr (0.3 at.%) single crystal before (1) and after (2) proton irradiation with a fluency of 10^{16} cm^{-2}.

with the Cr^{3+}(Nb) site while the second one arises from the Cr^{3+}(Li) site [16] (or reciprocal interpretation presented in [6] and [9]). The luminescence of the LN:Fe and LN:Cu crystals was not measured. But, taking into account the absorption measurements (2871 nm band) it may be assumed that in the case of these crystals Fe and Cu substitute Nb and also Li octahedral sites (see insert of Fig. 1).

Fig. 3 shows transmission (a) and absorption (b) changes in the undoped LN crystal under gamma, thermal and proton treatments. As one can see, annealing at 400°C (a.3) of the previously gamma 10^5 Gy irradiated LN sample (a.2) leads to relaxation of the transmission to the shape before irradiation (a.1). Next annealing treatments were performed at a higher (800°C) temperature and it is seen that the shape of transmission after 800°C annealing (a.5, a.7) significantly differs from the 400°C case (a.1, a.3). An increase in gamma dose (a.4 and a.6) leads to a saturation of transmission and absorption changes.

The effect of the 800°C annealing in Fig. 3a should be discussed more in detail and separately for the first and second 800°C treatment. The annealing was in each case performed after the irradiation and annealing treatments and correspond to the curves with lower numbers as described in the experimental section (e.g. curve 7 describes a sample with the sum of the treatments of 2 to 6). The first annealing increases the change due to the foregoing γ irradiation (Fig. 3a, curve 4) which is very surprising. The second annealing at 800°C does recover the effect of the irradiation with 10^7 Gy very incompletely. This might indicate that this strong radiation damage is hard to anneal.

As one can see from Fig. 3b proton irradiation gives almost the same changes in the absorption spectrum as in the case of gamma rays. From Fig. 3b it follows that in the additional absorption of $LiNbO_3$ single crystals irradiated with gamma rays and protons there arise at least two additional bands peaked at about 384 and 500 nm.

Irradiation of Fe, Cr and Cu doped LN crystals with gamma rays leads to some new, interesting changes in absorption. Annealing should generally restore optical features of each doped crystal previously gamma irradiated (see e.g. Fig. 4 curves 3, 6 and Fig. 5 curves 1, 4 and 3, 6). But for the dose of 10^5 Gy and 10^6 Gy we are dealing with an abnormally reduced absorption – (bleaching phenomenon, curves 2, 5). In the case of the LN:Fe crystal the annealing at 400°C for 3 h after 10^5 Gy irradiation does not restore the initial transmission (curves 1, 4) while 10^6 Gy irradiation (curve 2) and

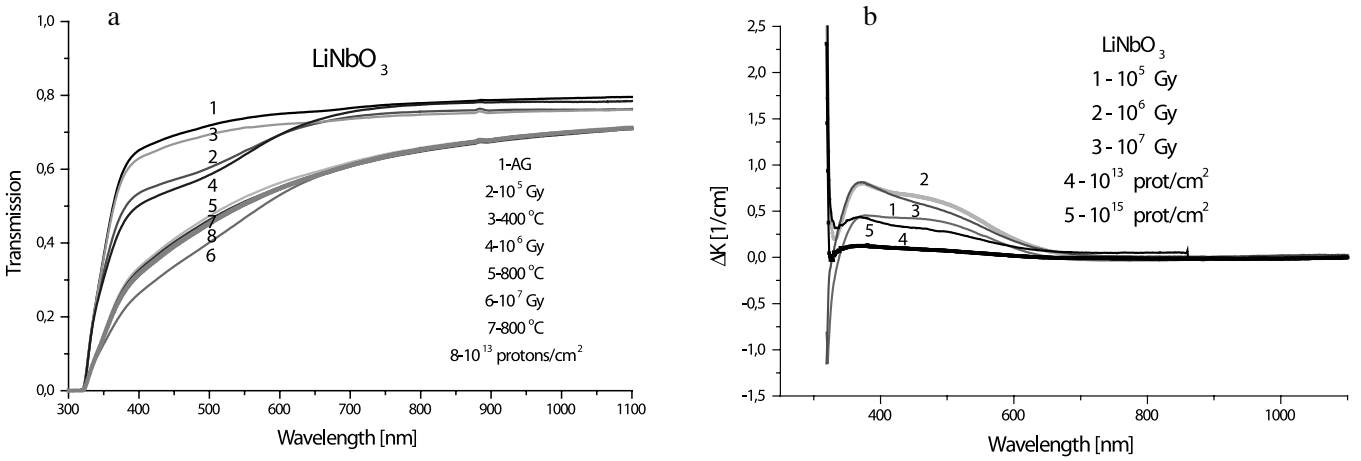

Fig. 3. Changes in the transmission (a) and absorption (b) after gamma and thermal treatments.

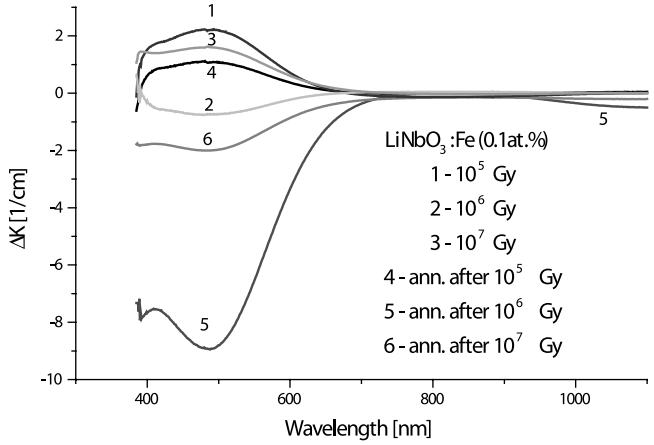

Fig. 4. Additional absorption in LN: Fe single crystals after gamma and thermal treatments.

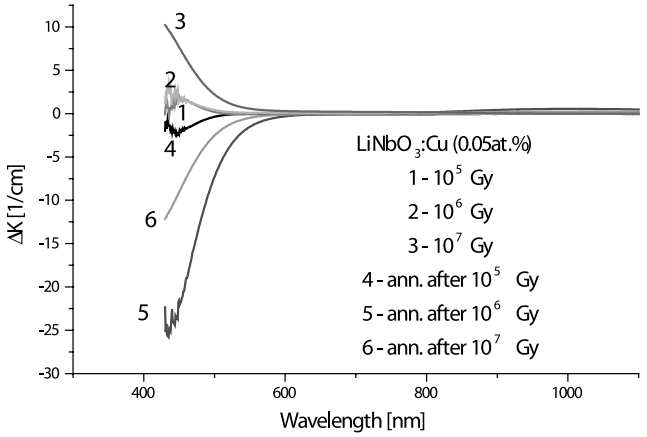

Fig. 5. Additional absorption in LN: Cu single crystals after gamma and thermal treatments.

800°C annealing for 3 h (curve 5) bleached the crystal. In the case of the LN:Cu samples, as one can see from Fig. 5, 10^6 Gy is a dose for which some saturation of the absorption change is observed (curve 2 as compare to curve 1) and bleaching occurs after 800°C annealing for 3 h (curve 5). With increasing dose up to 10^7 Gy a further increase of additional absorption is observed for both LN:Fe and LN:Cu crystals (Fig. 4 curve 3 and Fig. 5 curve 3).

In case of the LN:Cr crystal it was observed that the annealing at 400°C for 3 h also does not restore the initial transmission.

As one can see from Figs. 3, 4, 5 and 6, the shapes of the additional absorption of LN:Fe and LN:Cr crystals after gamma irradiation are almost similar as in the case of pure LN (excluding the relative intensity of the two mentioned bands), while the corresponding behavior of the LN:Cu crystal is significantly different. In the latter case, for doses up to 10^7 Gy, there is no 500 nm band observed. As shown in Fig. 6 a fitting procedure using Gauss curves gives at least four additional absorption bands peaked at 373, 402, 451 and 526 nm.

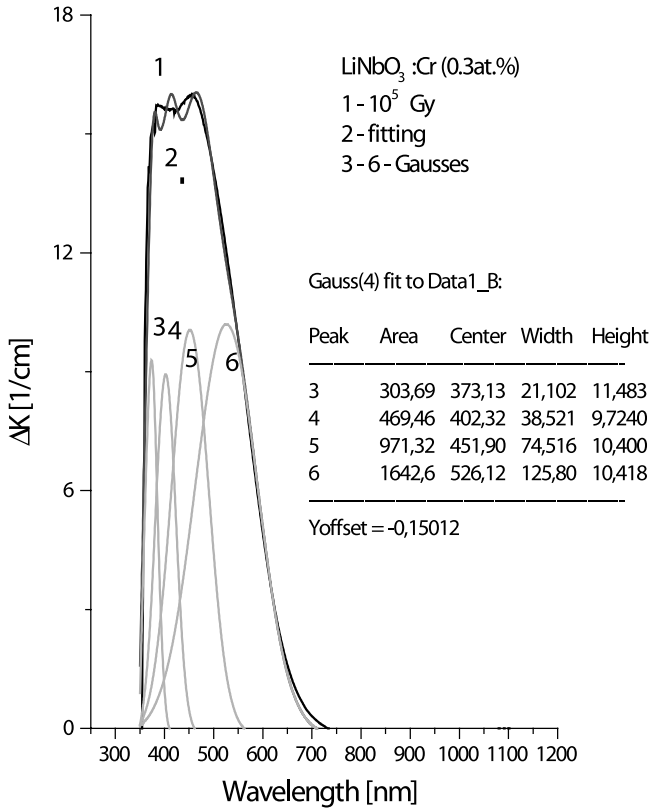

Fig. 6. Fitting procedure of the additional absorption in $LiNbO_3$:Cr single crystal after 10^5 Gy γ-rays using Gauss curves.

The different shape of the additional absorption after proton irradiation of the LN:Cu crystal with respect to other crystals is confirmed in Fig. 7, where changes in the absorption (mainly on the fundamental absorption edge and inside Cu^{2+} bands) after proton irradiation with fluences from 10^{13} cm^{-2} (2) to 10^{16} cm^{-2} (6) are shown. Subsequent curves describe the same sample absorption with respect to "as-grown" sample after subsequent fluences, so curve 6 describes LN:Cu sample, which was irradiated with protons with fluences: 10^{13}, 10^{14}, 10^{14}, 10^{15} and 10^{16} cm^{-2}. As one can see, only in the case of the high fluence of 10^{16} cm^{-2} there arises in the LN:Cu absorption spectrum an additional absorption at about 500 nm. In the fluence dependence of the additional absorption (b) at least three different behaviors are to be distinguished: one for fluences below 10^{14} cm^{-2}, one for fluences between 10^{14} and 5×10^{14} cm^{-2} and one for $> 5\times10^{14}$ cm^{-2}. The shape of this dependence is characteristic of the most investigated oxide crystals.

Fig. 8 presents photos of LN samples (pure – transparent white, Cu-doped – red-orange, and Fe-doped – red-brown samples) obtained after 10^{15} cm^{-2} proton irradiation. As one can see smaller effects are present in the pure LN crystal. This is important, because these effects change with time confirming relaxation processes taking place in the crystals.

Different behavior of LN:Cu samples was confirmed also by birefringence dispersion measurements. Fig. 9a–c presents changes in the polarimeter image (analyzer and polarizer were parallel) of $LiNbO_3$ wafers doped with Cu (0.06 at.% and 0.07 at.%). In the samples irradiated by protons one can see two crescents (b, c) which characterize the shape of the proton beam (it was focused). The contrast of the image is larger for higher doping (c). Moreover, the image changes with time due to a relaxation process. This means

that the above image is influenced also by color centers formed in the samples by protons.

Fig. 9d shows the horizontal cross-section of the BRD coefficient after irradiation with 10^{13} cm^{-2} protons of LN:Cu (0.07 at.%). One can see clear peaks correlated with the changes induced by the protons. Pure $LiNbO_3$ samples and samples doped with Fe and Cr (up to 0.3 at.%) did not exhibit such a strong effect for this fluence. For larger values of fluence (up to 10^{16} cm^{-2}) all these crystals clearly show a decrease in birefringence dispersion in the range of the proton beam intensity (see Fig. 9e–h).

Discussion

In contrast with stoichiometric crystals [4] in the absorption spectrum of LN:Cr, there was observed a 1260 nm (Fig. 1, curve 2) band associated probably with Cr^{4+} or Cr^{5+} absorption. In a Cr^{3+} doped lithium niobate congruent single crystal there were found Nb^{5+} sites in which substitution of an ion of higher than 3+ valency is possible [6]. But up to now nobody has measured luminescence of these centers. Fig. 1 clearly shows the possibile existence of higher than 3+ chromium ions absorption in LN crystals but we cannot find any evidence for it (luminescence investigations did not exhibit any emission). OH^- absorption seen in this Figure does not exclude substitution of both octahedral sites, Nb and Li, in all the investigated crystals. This fact was confirmed e.g. by luminescence measurements of R-lines in LN:Cr crystal (Fig. 2).

From Fig. 3a a very important property of LN crystals can be concluded: the optical characteristics is not stable with respect to temperature. It is possible that after growth of these crystals residual stresses remain. From this Figure it follows that annealing at 400°C and 800°C gives two different initial optical states (transmission curve). The dose dependence of the additional absorption after γ-irradiation observed in Fig. 3b (curves 1–3) suggests that in case of the pure LN crystal we deal with a saturation phenomenon with respect to radiation defects. No further increase in additional absorption (or in the amount of radiation defects) takes place when a dose of 10^6 Gy is exceeded. It means that for this value all point defects existing in the crystal (of the order of about 10^{17} cm^{-3}) are recharged by gammas. The shape of the additional absorption exhibits the presence of at least two bands, one of which being connected with F-type color centers (384 nm). The second one (500 nm) seems to be associated with Nb^{4+}-Nb^{4+} bipolarons described recently in [13] for reduced $LiNbO_3$. This is confirmed by the absorption of a pure non-irradiated LN crystal where a weak 500 nm band is also observed. Moreover, dissociation of these centers is observed after annealing giving additional absorption near 650 nm (polarons Nb^{4+}). The additional absorption of a LN crystal after proton irradiation, presented in Fig. 3b (curves 4, 5), shows the same features as previously found for gamma irradiation. It means that in the case of protons irradiation of LN crystals, for fluences below 10^{15} cm^{-2}, the dominating radiation efect is recharging of point defects existing after growth. This may be ionization of lattice and impurity ions and/or recombination of these ions with delta electrons formed by protons [12].

Other investigated crystals exhibit similar shapes of the additional absorption differing only by the magnitude of the additional absorption (greater for LN:Cr – 16 cm^{-1}, smaller for LN:Fe – 2 cm^{-1}) and the relative intensity of the two above mentioned peaks (384 and 500 nm).

Changes in the additional absorption of LN:Fe and LN:Cu single crystals due to gamma irradiation and thermal annealing (Figs. 4 and 5) confirm the discussed instability of optical properties against thermal treatment observed for pure LN (Fig. 3a). The only difference is that in the case of the former crystals one can observe some critical dose of γ-rays (10^6 Gy) for which drastic bleaching in absorption is observed. It may be due to residual stresses annealed by γ-rays. Comparing Figs. 4 and 5 one can see that the shape of the additional absorption differs significantly for both crystals, LN:Fe and LN:Cu. In the case of LN:Cu crystals there is no bipolaron band observed peaked at about 500 nm. The 460 nm additional absorption band seems to be connected mainly with Cu^+ ions formed by recharging of Cu^{2+} ($Cu^+ \rightarrow Nb^{5+}$ inter-

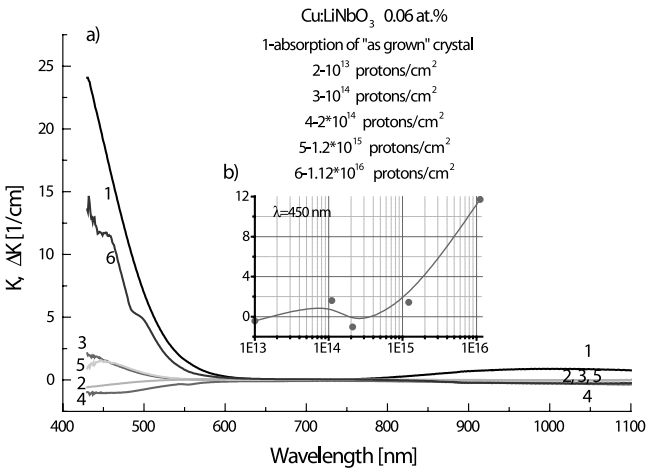

Fig. 7. Absorption (1) and the additional absorption (2–6) of LN:Cu single crystal after proton irradiation with fluences 10^{13}–10^{16} prot/cm^2 – a and fluency dependence of additional absorption in this crystal – b.

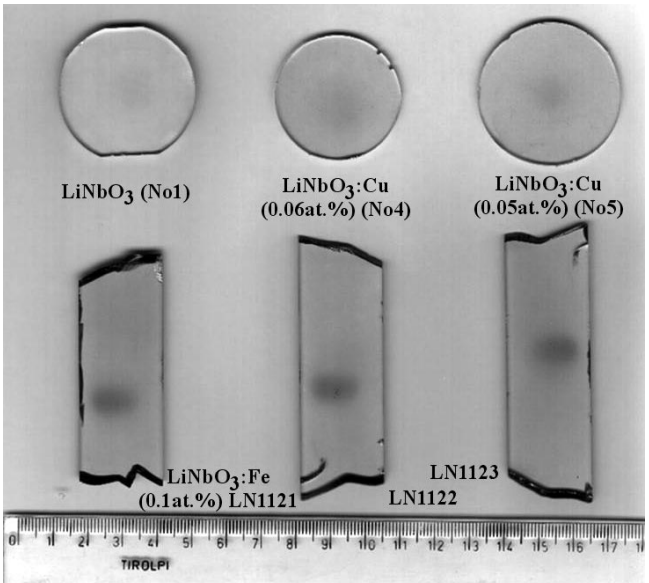

Fig. 8. Lithium niobate wafers (LN pure (white circle crystal), Cu doped (red-orange circle crystals), and Fe doped (red-brown rectangular crystals) after proton irradiation with a fluency of 10^{15} cm^{-2}.

valence transfer). Such supposition is confirmed by the corresponding changes in the 1000 nm Cu^{2+} band. This may be the reason why the 500 nm band is absent.

The detailed analysis of the shape of the additional absorption performed for LN:Cr (Fig. 6) has not shown two but four bands which are responsible for this absorption. The first two bands are well known F^+ and F centers [7]. The third band indicates an increase in the Cr^{3+} absorption. It may be due to e.g. recombination of Cr^{4+} ions with Compton electrons. The fourth band is associated with bipolarons Nb^{4+}-Nb^{4+}. In the case of LN:Fe crystals the third band, centered at about 480 nm, reveals an increase in Fe^{2+} absorption. This supposition is confirmed by the corresponding changes observed for the magnitude of 1062 nm absorption after gamma (increase) and annealing (decrease) treatments.

Fig. 7 presents a characteristic shape of the additional absorption for all the investigated LN:Cu crystals and the fluence dependence in the case of proton irradiation of LN:Cu single crystal. The fluence dependence of the addi-

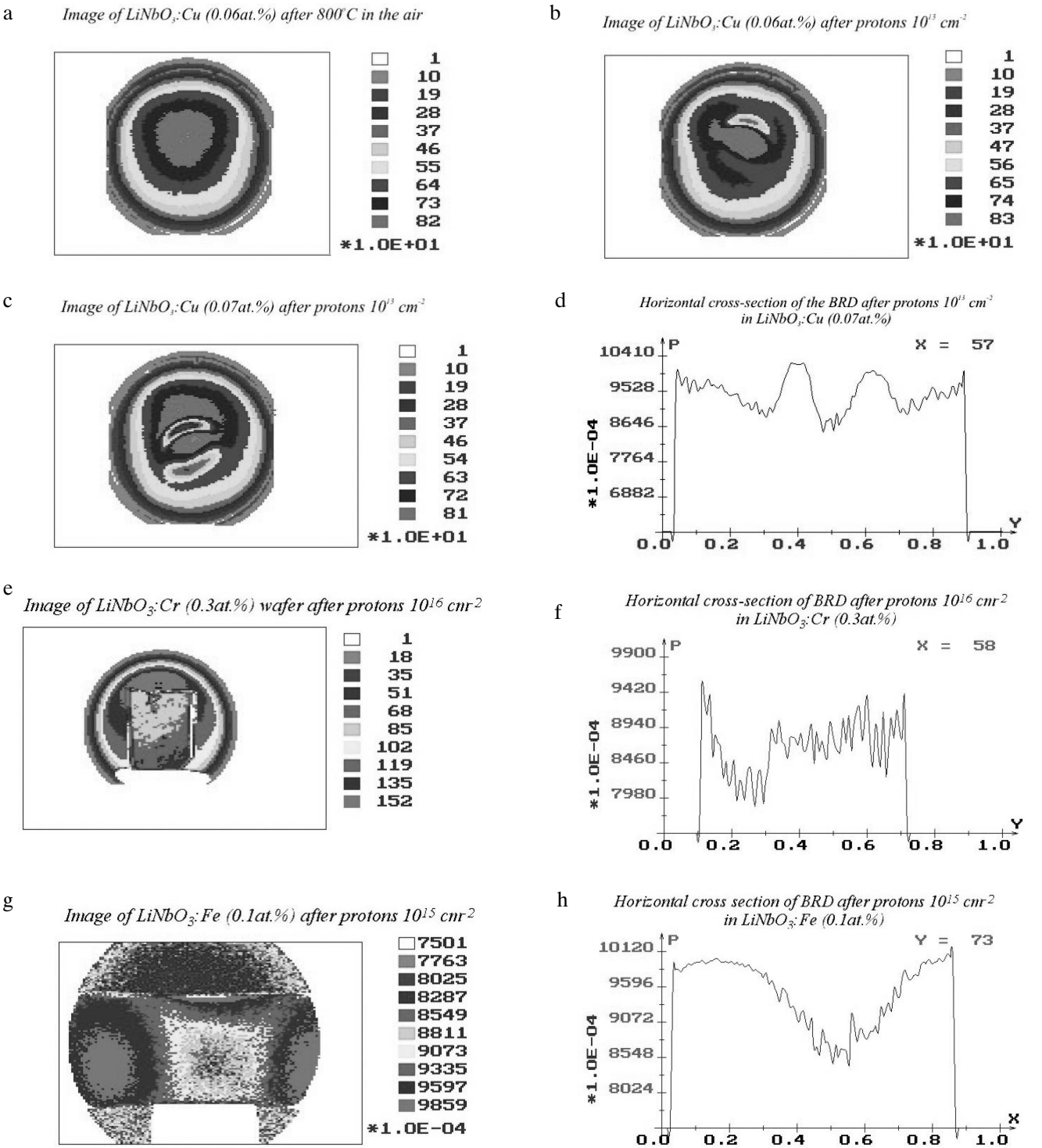

Fig. 9. Images of LN:Cu (0.06 at.%) – (a, b) and LN:Cu (0.07 at.%) – (c) samples before (a) and after (b, d) proton irradiation with a fluence of 10^{13} cm^{-2}; horizontal cross-section of the BRD coefficient (eq. 2) after protons 10^{13} cm^{-2} in LN:Cu (0.07 at.%) – (d); image of LN:Cr (0.3 at.%) sample (rectangle) after 10^{16} protons/cm^2 – (e) and horizontal cross-section of the BRD coefficient for this crystal – (f); image of LN:Fe (0.1 at.%) sample (rectangle) after 10^{15} protons/cm^2 – (g) and horizontal cross-section of the BRD coefficient for this crystal – (h).

tional absorption exhibits a characteristic shape with a maximum at about 10^{14} cm^{-2}, a minimum at about 10^{15} cm^{-2} and a further sharp rise for higher fluences. The monotonic increase of the additional absorption up to 10^{14} cm^{-2} is associated with recharging processes of point defects. The probable reason of the decrease of the additional absorption in the region 10^{14} cm^{-2}–10^{15} cm^{-2} could be a mutual interaction of the cascades from different proton trajectories [11]. A strong increase of the additional absorption above 10^{15} cm^{-2} is characteristic of Frenkel defect formation. Also in the case of proton irradiation LN:Cu crystal differs from others. Especially the additional absorption characteristics for Nb^{4+}–Nb^{4+} bipolarons arises only for a fluence as high as 10^{15} cm^{-2}.

Luminescence measurements of a LN:Cr crystal at low temperatures have shown that proton irradiation leads to a change in relative luminescence intensity from $Cr^{3+}(Nb^{5+})$ and $Cr^{3+}(Li^{+})$ sites. We observe an increase in luminescence associated with the latter one (see Fig. 2).

Polarimetric measurements (Fig. 9b-d) have shown that the LN:Cu crystal exhibits strong susceptibility to proton irradiation. Even for such small fluencies as 10^{13} cm^{-2}, the observed changes in the polarimetric image and the BRD coefficient are very significant. Moreover, there are not only due to color centers (investigations were performed for λ = 670 and 760 nm), but also due to some other changes, e.g. in band gap. Similar investigations were performed for gamma irradiated and thermally annealed samples. It has been observed rather unexpectedly that thermal annealing can lead to a decrease in optical homogeneity in the majority of all cases. This may be attributed to the generation of an internal electric field by the pyroelectric effect, and to the electrooptic effect involved thereafter. The secondary electrons which are homogeneously generated by gamma irradiation in the investigated crystals are believed to increase the optical homogeneity, also by compensating this field.

Birefringence dispersion seems to be a good key parameter in the manufacture of e.g. retardation plates, 2nd harmonic generators or polarizers.

Acknowledgments The author would like to thank Miss I. Pracka, Mrs M. Świrkowicz and A.L. Bajor from ITME for the investigated crystals and measurements of birefringence, Miss J. Wojtkowska from Soltan IPJ Świerk for proton irradiations, Miss T. Wrońska from IChTJ for gamma irradiations and Miss A. Kamińska from IF PAN for luminescence measurements.

References

1. Arizmendi L, Cabrera JM, Aguillo-Lopez F (1984) Defects induced in pure and doped $LiNbO_3$ by irradiation and thermal reduction. J Phys C: Solid State Phys 17: 515–529
2. Bajor AL (1998) Testing of optical materials by birefringence dispersion mapping. In: Nijhawan OP *et al.* (ed) Optics and optoelectronics. Theory, devices and applications, vol. 2. Narosa Publishing House, New Delhi-Madras-Bombay-Calcutta-London, pp 1312–1316
3. Clark MG, DiSalvo FJ, Glass AM, Peterson GE (1973) Electronic structure and optical index damage of iro-doped lithium niobate. J Chem Phys 59;12:6209–6219
4. Corradi G, Sothe H, Spaeth JM, Polgar K (1991) Electron spin resonance and electron-nuclear double-resonance investigation of a new Cr^{3+} defect on an Nb site in $LiNbO_3$:Mg:Cr. J Phys: Condens Mat 3:1901–1908
5. Crawford JH Jr (1984) Defects and defects processes in ionic oxides: where do we stand today? Nucl Instrum Meth B1 229:2–3:159–173
6. Garcia-Sole J, Macalik B, Bausa LE et al. (1993) Optical detection of ion impurity sites in doped $LiNbO_3$. J Electrochem Soc 140;7:2010–2015
7. Hughes AE, Henderson B (1972) In: Crawford JH, Slifkin LM (eds) Point defects in solids. Plenum Press, New York-London, pp 381–386
8. Jabłoński R, Kaczmarek SM, Pracka I, Surma B, Świrkowicz M, Łukasiewicz T (1998) ESR and optical measurements of $LiNbO_3$ and $LiTaO_3$ single crystals doped with ions of the first transition series. Spectrochim Acta A 54:1701–1709
9. Jaque F, Garcia-Sole J, Camarillo E, Lopez FJ, Murietta H, Hernandez J (1993) Detection of Cr^{3+} sites in $LiNbO_3$:MgO, Cr^{3+} and $LiNbO_3$:Cr^{3+}. Phys Rev B 47;9:5432–5434
10. Kaczmarek SM, Jabłoński R, Pracka I, Świrkowicz M, Wojtkowska J, Warchoł S (1999) Radiation defects in $LiNbO_3$ single crystals doped with Cr^{3+} ions. Cryst Res Technol 34:729–735
11. Kaczmarek SM, Wojtkowska J, Moroz Z, Kisielewski J (1999) Interaction of protons with oxide compounds. In: Sangwal K (ed) 3rd Int Conf on Intermolecular Interactions with Matter. University of Technology, Lublin, pp 148–152
12. Kaczmarek SM, Wojtkowska J, Moroz Z, Pracka I (1999) Valency change of impurities inside oxide compounds under proton irradiation. J Alloys Compd 286;1–2:167–173
13. Koppitz J, Schirmer OF, Kuznetsov AI (1987) Thermal dissociation of bipolarons in reduced undoped $LiNbO_3$. Eur Phys Lett 4;9:1055–1059
14. Kotomin EA, Popov AI (1998) Radiation-induced point defects in simple oxides. Nucl Instrum Meth B 141:1–15
15. Malovichko GI, Grachev VG, Schirmer OF (1994) The effect of iron ions on the defect structure of lithium niobate crystals grown from K_2O containing melts. Solid State Compd 89:195–198
16. Nicholls JFH, Han TPJ, Henderson B, Jaque F (1993) Charge compensation and site-selective luminescence of Cr^{3+}:$LiNbO_3$. Chem Phys Lett 202;6:560–567
17. Petrosjan AK, Hachatrian RM, Sharojan EG (1984) Effekt Jahna-Tellera jona Cu^{2+} w monokrystalle $LiNbO_3$. Fizika Tvordogo Tela 26;1:22–28
18. Polgar K, Peter A, Kovacs L, Corradi G, Szaller Zs (1997) Growth of stoichiometric $LiNbO_3$ single crystals by top seeded solution growth method. J Cryst Growth 177:211–216
19. Pracka I, Bajor A, Kaczmarek SM, Świrkowicz M, Kaczmarek B, Kisielewski J, Łukasiewicz T (1999) Growth and characterization of $LiNbO_3$ single crystals doped with Cu and Fe ions. Cryst Res Technol 34:627–634